Self-Assembly

DOI: 10.1002/ange.201302177

Unidirectional Scaffold-Strand Arrangement in DNA Origami**

*Dongran Han, Shuoxing Jiang, Anirban Samanta, Yan Liu, and Hao Yan**

Since the origin of DNA nanotechnology over 30 years ago, branched DNA tiles have been developed to construct a variety of DNA nanostructures. Among the unique building blocks that have been demonstrated, rigid, antiparallel double-crossover (DX) tiles[1] have had great significance as both the unit motif in the first two-dimensional DNA crystal reported and as the basic repeating unit in most DNA origami structures.[2–17] In contrast, parallel DX tiles have yet to be developed, despite that they were initially reported more than 20 years ago, most likely because their assembly yields are not comparable to anti-parallel DX tiles. Herein we demonstrate construction of DNA origami architectures based on modified parallel DX tiles, in which a single-crossover linkage, rather than reciprocal crossovers, is present at each junction point between neighboring helices. The yields of these novel origami structures are similar to their counterparts that are constructed based on antiparallel DX tile units containing double-reciprocal crossovers at each junction point. We demonstrate that a unidirectional arrangement of the scaffold strand can be used in the assembly of a variety of 2D and 3D DNA origami. This new design will greatly expand the diversity of DNA origami achieved and enable their further assembly into larger structures.

The DX tiles, defined by Fu and Seeman in 1993, each contain two independent crossover points that join two adjacent DNA helices to form a rigid tile with the axes of the helices between the crossovers arranged roughly coplanar. Five types of DX tiles were initially reported: two antiparallel and three parallel molecules that differed in the relative orientation of the helical domains, the arrangement of the constituent strands, and the distance between the crossover points.[1] DAE and DAO molecules (double-crossover antiparallel molecules with an even number or odd number of half turns between crossover points along the same two helices) were later applied to DNA origami designs with great success, largely because these tiles contain two unperturbed DNA strands of opposing polarity that are easily linked to form a scaffold strand. In that case, the antiparallel scaffold is wound back and forth in a raster fill pattern to form a particular shape, through the use of hundreds of staple strands.[5] In contrast, DPE (double-crossover parallel molecules with an even number of half turns between crossover points) molecules were not thoroughly explored for the construction of higher-order structures. Compared to antiparallel DX molecules, parallel DX molecules are generally regarded as less stable presumably because of stronger electrostatic repulsion between the opposing DNA backbones.[1] Later, Sherman and co-workers reported that strand end-pinning and misfolding caused by the structural bias of nominally flexible junctions might affect the proper structural formation of parallel DX molecules.[18]

Breaking the continuity of one of the two strands that comprise each junction in a DPE tile at the junction point will produce parallel, double-helical units with single-crossover linkages between the helices. Such modified DPE tiles provide a direct solution to both the possible steric hindrance at the crossover points and the kinetic trap noted by Sherman and co-workers.[18] Herein, we demonstrate that the unperturbed strands in these modified DPE tiles can be linked to form a long scaffold strand that is directed by a collection of staple strands to form DNA origami structures. The scaffold strand in adjacent helices possesses the same 5′–3′ polarity and we therefore refer to these structures as parallel helix (PH) origami. Assembling PH origami required that we develop unique, coiled-scaffold folding paths rather than the typical raster fill patterns adopted by the scaffold in DNA origami structures with antiparallel helices (AH). We also designed and assembled hybrid DNA origami structures that contain both parallel and antiparallel scaffold regions.

The DAE, DPE, and modified DPE tiles are shown in Figure 1 A–C for comparison. The single-stranded DNA (depicted in gray) remains unperturbed at all junction points and the relative polarities of these two strands determine whether the molecules are classified as antiparallel or parallel. The remaining DNA strands are shown in various colors and correspond to the staple strands that direct/hold the linear strands in a coplanar arrangement. The staple strands in the antiparallel tiles (Figure 1 A) reverse direction at each crossover point while those in the parallel tiles (Figure 1 B) do not. Note that the backbones of the strands at the crossover points in the parallel tiles are directly opposite one another, which imparts a certain degree of instability to the parallel tiles. Thus, in the modified DPE tiles (Figure 1 C), a single-crossover linkage replaces the typical reciprocal

[*] Dr. D. Han, S. Jiang, A. Samanta, Prof. Y. Liu, Prof. H. Yan
The Biodesign Institute, Arizona State University
Tempe, AZ 85287 (USA)
E-mail: hao.yan@asu.edu
Dr. D. Han, S. Jiang, A. Samanta, Prof. Y. Liu, Prof. H. Yan
Department of Chemistry and Biochemistry
Arizona State University
Tempe, AZ 85287 (USA)

[**] This work is supported by a National Science Foundation grant (1104373), an Office of Naval Research grant (N000140911118), an Army Research Office grant (W911NF-11-1-0137) to H.Y. and Y.L., and an Army Research Office MURI award (W911NF-12-1-0420) to H.Y. H.Y. and Y.L. are part of the Center for Bio-Inspired Solar Fuel Production, an Energy Frontier Research Center funded by the U.S. Department of Energy, Office of Science, Office of Basic Energy Sciences under Award Number DE-SC0001016. H.Y. is supported by the Presidential Strategic Initiative Fund from Arizona State University.

Supporting information for this article is available on the WWW under http://dx.doi.org/10.1002/anie.201302177.

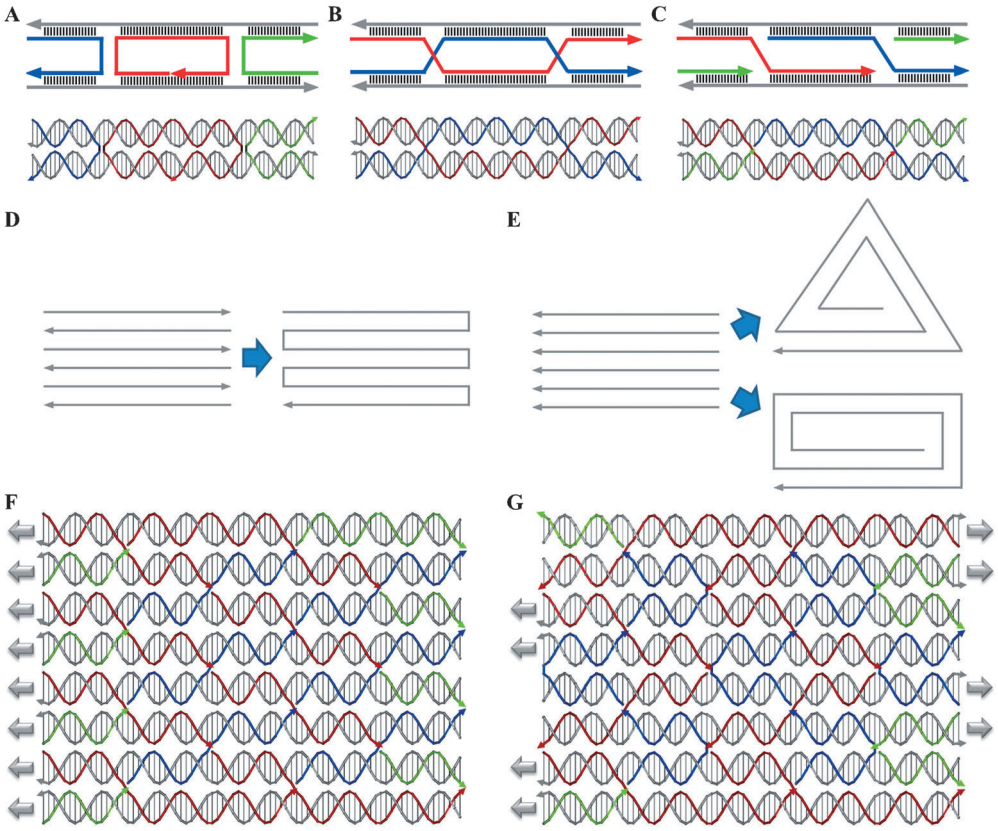

Figure 1. PH DNA origami designs: A) DAE tile; B) DPE tile; C) modified DPE tile with single-crossover linkages. All three have three full helical turns (32 bp) between adjacent crossover points. Gray strands are the unperturbed linear strands and the colored strands are the staples strands. Arrowheads indicate the 3′ end of each DNA strand. D) Adjacent antiparallel strands are linked to form raster fill patterns. E) Parallel strands can be linked to form coiled patterns. F) A selected portion of a PH DNA origami design. G) A selected portion of a DNA origami design containing both parallel and anti-parallel scaffold regions. The staple stands between parallel and antiparallel linkages are shown in red and blue, respectively.

crossovers, reducing the steric hindrance of the DNA backbones at the junctions.

When the unperturbed gray strands in the mutated DPE tiles are linked together to form a scaffold, the track of the scaffold strand will be different from that present in traditional AH origami. For the DAE-based origami structures, a raster fill scaffold pattern ensures an antiparallel polarity among all adjacent strands (Figure 1D). Conversely, in the PH DNA origami, the adjacent scaffold strand domains must remain in parallel throughout the entire structure. To meet this requirement, we employed a coiled folding strategy for the scaffold strand; two examples of the resulting paths are shown in Figure 1E. After each round of the folding path, the scaffold strand loops back with the same polarity as the adjacent previous layer.

A representative PH DNA origami structure (local) with detailed design information is presented in Figure 1F. The gray arrows on the left side of the structure denote the 5′ to 3′ polarity of the scaffold strand in the helices. Note that there are two single-crossover linkages between all adjacent helices in this structure. In the figure, the staple strands that traverse downward between helices from 5′ to 3′ are depicted in red and those that traverse upward between helices from 5′ to 3′ are depicted in blue. The staple strands shown in green do not traverse between helices and thus do not participate in any crossovers.

We also demonstrated that PH DNA origami designs are fully compatible with AH DNA origami. We assembled a structure in which the scaffold strand adopted both parallel and antiparallel arrangements. Figure 1G illustrates the design of a hybrid origami structure in which adjacent scaffold sections alternate between the two polarities. For instance, the scaffold strand in the first and the second helices are parallel to one another; those in the second and the third helices are anti-parallel; and those in the third and fourth helices are parallel, and so on.

Circular single-stranded M13 DNA was used as the scaffold strand in all designs presented herein to evaluate the feasibility of this unconventional design strategy and new scaffold folding paths. Four basic two dimensional (2D) structures, including two rectangles, one triangle and one square, were designed and constructed. Figure 2 shows the design schemes and the corresponding AFM images of the four unique PH DNA origami objects. The polarities of the DNA helices are represented by unique colors with the 5′ to 3′ directionality shown as moving from red to purple in the models. M13 DNA is a closed single-stranded DNA loop. In the rectangular design shown in Figure 2A the parallel scaffold-strand path was realized by leaving some single-stranded loops on both sides of the rectangle. Notice that there is a gap in the center of the design (Figure 2A second row) that represents an antiparallel connection between the two halves of the helical domains. The compatibility of PH and AH origami is demonstrated by the second rectangular design shown in Figure 2B, where the polarity of the helices are arranged as shown in Figure 1G. In this design, every helix is flanked by one parallel and one antiparallel helical row, with the exception of the top- and bottom-most helices. Again, single-stranded loops were included on both sides of the structure to meet the design requirements. Because of the presence of these loops, the edges of both of the rectangular designs appear rough in the AFM images.

Polygonal shapes, such as squares and triangles, are easily constructed from a coiled folding pattern (Figure 2C,D). In

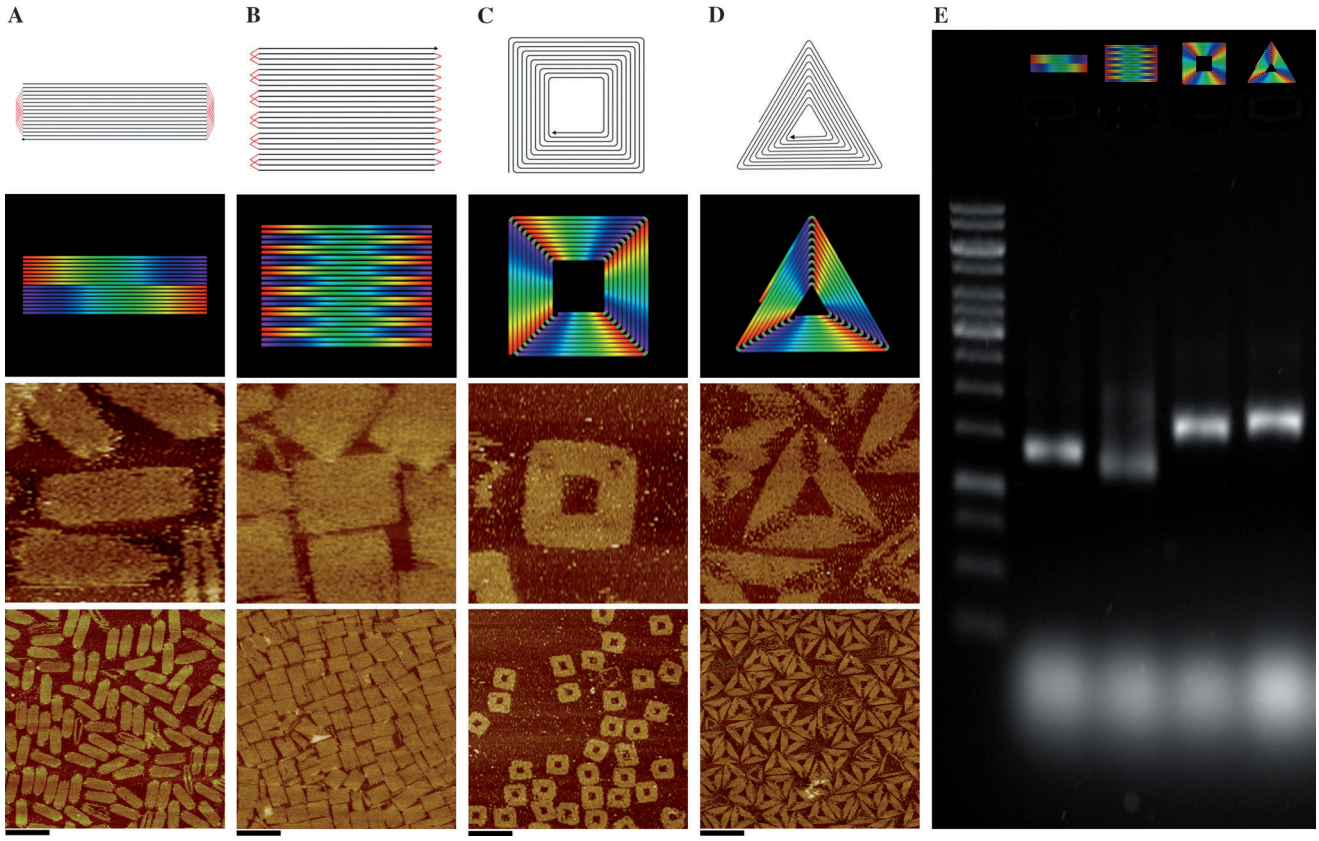

Figure 2. 2D PH DNA origami structures: A) Rectangle; B) AH-PH hybrid rectangle; C) square; D) triangle. Top) the folding path of the scaffold strand with the arrows pointing to the 3′ end. Red = single-stranded loops. Second row) polarity of different regions of the structure: 5′ ends are red changing to purple at the 3′ ends. Third row) zoomed AFM images of the assembled structures, each 200 nm × 200 nm. Bottom) AFM images of the assembled structures. Scale bars = 200 nm. E) Agarose gel (0.75 %) characterization of the PH (and PH-AH hybrid) origami nanostructures.

both of these designs all of the adjacent helical rows exhibit parallel polarity. One important observation is the high yields of all four basic PH (or hybrid PH/AH) origami structures, based on the AFM images, without any purification, close to those of the corresponding AH origami.

In addition to simple 2D shapes, PH origami can adopt complex topological structures and 3D shapes, like their AH origami counterparts. Figure 3 A shows the design of a topologically complex PH origami (left) of a "figure eight" and the corresponding TEM characterization of the assembled structures (right). According to our design, the crossing arms in this figure eight are expected to adopt either a left-handed or right-handed conformation. However, in the TEM images most of the well-formed structures exhibit a right-handed conformation. Some twisting of the structures without an overlapping cross in the center of the figure eight was also observed. These unexpected results are likely because of intrinsic tension in the design (see the Supporting Information for discussion).

Figure 3 B,C demonstrate the successful design and assembly of two PH origami screws of different diameters. This winding helical pattern can be easily applied to any screw shaped structures. The screw in Figure 3 B has a diameter of approximately 7.4 nm and a length of about 113 nm. The screw in Figure 3 C has a diameter of approximately 9.0 nm and a length of around 100 nm. For the screw designs we expected to find both left- and right-handed conformations, however, that level of structural detail was difficult to extract from the TEM images. We did observe that the screw-shaped structures tend to form dimers, which could be caused by sharing staples strands between two structures or the interactions between the single-stranded loops that are required to connect the two ends of the screw.

In summary, we designed and assembled DNA origami structures with the scaffold strand between adjacent helices arranged unidirectionally. The modified DPE tiles used in the PH DNA origami are stable enough to assemble various structures, with yields comparable to those assembled from DAE/DAO units. Coiled helical fill patterns were adopted in the PH origami structures, and a combination of parallel and antiparallel scaffold domains in a single structure was also realized. The design strategy presented herein expands the diversity of structures achievable using DNA origami.

As noted above, we used circular M13 DNA for all PH origami construction, which is the same as most previously reported AH origami structures. In the two rectangular-shaped PH origami structures, several single-stranded scaffold regions were used to bridge the gap between distant binding regions to maintain the parallel arrangement of the scaffold strand. For all the other structures reported herein, only one single-stranded scaffold region was used to link the two ends of the scaffold strand (see Supporting Information, Figures S5-1–S5-7 for illustration of the ssDNA regions in our designs). Linear scaffolds can certainly be applied to the PH

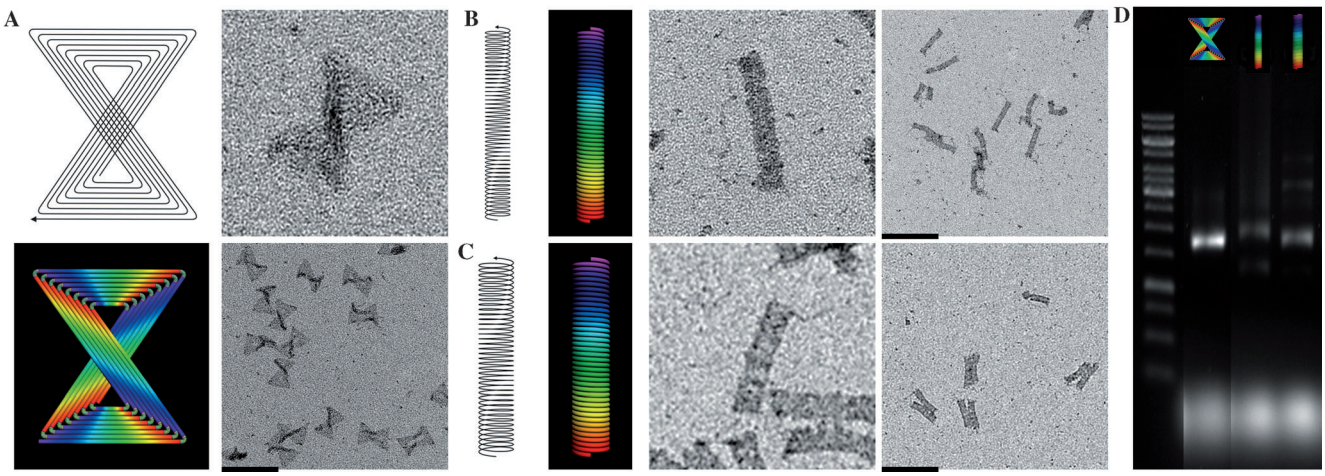

Figure 3. 3D PH DNA origami structures: A) Top, left: simplified views of the folding path of the scaffold strand. Arrows point to the 3′ end of the scaffold. Bottom, left: red corresponds to the 5′ end of the scaffold and purple the 3′ direction. Right: TEM images of the assembled structures. B,C) Screw-shaped origami with diameters of approximately 7.4 nm and 9.0 nm, respectively (left), and TEM images of the assembled structures (right). Zoomed images are 200 nm × 200 nm. Scale bars = 200 nm. D) Agarose gel (0.75 %) characterization of the PH origami nanostructures.

origami strategy, and it should be noted that the single-stranded regions do not facilitate the formation of PH origami structures. On the contrary, they can be considered as inert domains that merely ensure a continuous M13 arrangement in the design. For example, it would be better to use a linear scaffold (rather than a circular one) to construct the screw shaped origami because it is likely that the ssDNA that links the two ends of the screw will cause unwanted deformation or cross-linking (to form dimers). Figure S6 shows AFM images of two PH origami structures (square and rectangular) constructed from a linear M13 scaffold, without any purification. Because it takes more steps (e.g. exonuclease digestion) to prepare linear M13 and there is not much advantage to using the linear scaffold to construct the PH origami, we decided not to systematically look into the use of linear scaffolds for our design.

One of the most important challenges for DNA nanotechnology is to construct randomly shaped objects with exquisite control over the morphology of the product (regardless of the construction method); PH origami represents a valuable and novel addition to the construction DNA origami structures. For example, the double-helical DNA that is coiled around histone proteins adopts a left-handed orientation, and a PH design strategy is ideal for constructing similar structures. The PH origami can also be easily integrated with mechanical DNA nanodevices built from paranemic crossover motifs[19,20] to increase the complexity of DNA device functions. While an antiparallel arrangement of the scaffold strand will not permit the formation of certain designs (such as the screw-shaped origami demonstrated here), the PH origami design strategy can be used, providing a sound alternative in certain situations. Another potential advantage of the PH design strategy is that with this new design principle researchers can now connect edges of the DNA origami structures or smaller tiles with both parallel and antiparallel scaffold arrangements using staple strands, which is a commonly encountered issue when programming interactions between DNA origami structures. Given the pace with which DNA nanotechnology is moving forward, new building blocks are sure to facilitate progressive developments in the fields of nano-construction and biomimicry.

Received: March 14, 2013
Revised: June 16, 2013
Published online: July 14, 2013

Keywords: DNA nanotechnology · DNA origami · nanostructures · parallel DNA crossover · self-assembly

[1] T. J. Fu, N. C. Seeman, *Biochemistry* **1993**, *32*, 3211 – 3220.
[2] E. Winfree, F. Liu, L. A. Wenzler, N. C. Seeman, *Nature* **1998**, *394*, 539 – 544.
[3] P. W. K. Rothemund, N. Papadakis, E. Winfree, *PLoS Biol.* **2004**, *2*, e424.
[4] F. Mathieu et al., *Nano Lett.* **2005**, *5*, 661 – 665.
[5] P. W. K. Rothemund, *Nature* **2006**, *440*, 297 – 302.
[6] Y. He et al., *Nature* **2008**, *452*, 198 – 201.
[7] R. D. Barish, R. Schulman, P. W. K. Rothemund, E. Winfree, *Proc. Natl. Acad. Sci. USA* **2009**, *106*, 6054 – 6059.
[8] E. S. Andersen et al., *Nature* **2009**, *459*, 73 – 76.
[9] S. M. Douglas, et al., *Nature* **2009**, *459*, 414 – 418.
[10] Y. Ke et al., *J. Am. Chem. Soc.* **2009**, *131*, 15903 – 15908.
[11] H. Dietz, S. M. Douglas, W. M. Shih, *Science* **2009**, *325*, 725 – 730.
[12] Y. Ke, et al., *Nano. Lett.* **2009**, *9*, 2445 – 2447.
[13] T. Liedl, B. Högberg, J. Tytell, D. E. Ingber, W. M. Shih, *Nat. Nanotechnol.* **2010**, *5*, 520 – 524.
[14] D. Han, S. Pal, Y. Liu, H. Yan, *Nat. Nanotechnol.* **2010**, *5*, 712 – 717.
[15] D. Han, et al., *Science* **2011**, *332*, 342 – 346.
[16] Y. Ke, N. V. Voigt, K. V. Gothelf, W. M. Shih, *J. Am. Chem. Soc.* **2012**, *134*, 1770 – 1774.
[17] B. Wei, M. Dai, P. Yin, *Nature* **2012**, *485*, 623 – 627.
[18] M. T. Kumara, D. Nykypanchuk, W. B. Sherman, *Nano Lett.* **2008**, *8*, 1971 – 1977.
[19] H. Gu, J. Chao, S. J. Xiao, N. C. Seeman, *Nat. Nanotechnol.* **2009**, *4*, 245 – 248.
[20] H. Gu, J. Chao, S. J. Xiao, N. C. Seeman, *Nature* **2010**, *465*, 202 – 205.